The Second CIRP Conference on Biomanufacturing

Viscoelastic properties of rapid prototyped magnetic nanocomposite scaffolds for osteochondral tissue regeneration

Roberto De Santis[a,*], Antonio Gloria[a], Teresa Russo[a], Alfredo Ronca[a], Ugo D'Amora[a], Giacomo Negri[b], Dante Ronca[c], Luigi Ambrosio[d]

[a]Institute of Polymers, Composites and Biomaterials, National Research Council of Italy, V. le J.F. Kennedy, 54, 80125 Naples, Italy.
[b]Villa Betania Evangelical Hospital, Via Argine,604, 80147 Naples, Italy.
[c]Institute of Orthopaedics and Traumathology, II University of Naples, Via L. De Crecchio, 2-4, 80138 Naples, Italy.
[d]Department of Chemical Science and Materials Technology, National Research Council of Italy, Piazzale Aldo Moro 7, 00185 Roma, Italy

* Corresponding author. Tel.: +39-081-242536; fax: +39-081-2425932. E-mail address: rosantis@unina.it

Abstract

Poly(ε-caprolactone) and poly(ethylene glycol) based magnetic nanocomposite scaffolds were fabricated using fused deposition modeling and stereolithography approaches, and a hybrid scaffold was obtained by combining these additive manufacturing technologies. Viscoelastic properties in compression were investigated at 37°C, spanning a range frequency of four decades. Results suggest that poly(ε-caprolactone) and poly(ethylene glycol) based scaffolds adequately reproduce viscoelastic properties of subchondral bone and articular cartilage tissues, respectively. By combining fused deposition modeling and stereolithography it is possible to manufacture a hybrid scaffold suitable for osteochondral tissue regeneration.

1. Introduction

Osteoarthritis represents the most common joint disorder causing severe pain and disability [1,2]. This pathology damages subchondral bone and cartilage, and total joint arthroplasty (e.g., knee and hip prostheses) is still the choice for the treatment of the late stage osteoarthritis [3,4]. Metals, ceramics, polymers and composites are the materials used to fabricate these prostheses [4-7], and often acrylic cements [8,9] are used to fix the prosthesis to bone. However, due to several drawbacks of prosthetic devices, revision of an implanted prosthesis is required [10]. In this scenario, osteochondral bone regeneration represents a great challenge.

A scaffold for tissue engineering has to satisfy several requirements: an interconnected porous architecture able to promote cell-material interaction and extracellular matrix deposition; withstand the forces acting on the bone-joint segment and transfer the stress to the hosting tissue allowing the mechanical stimulation of tissue cells; tailored mechanical and degradation properties in order to gradually transfer the loading function to the newly forming tissue [11-17]. In particular, polymer-based composite materials can be designed to achieve enhanced functional and mechanical properties [7,15,16,18]. Benefiting from the large variety of biocompatible polymers, spanning from cross-linked networks to weak gels, scaffolds may be designed in the form of solid-like [15-22], strong gel-like [23-25] or injectable [26-30] formulations according to the specific application. Advanced scaffolds for tissue engineering able to release, *in situ*, drugs or cells could be obtained by integrating different technologies, also involving several strategies to improve cell attachment (i.e., surface functionalization) [30-35].

Different approaches have been proposed to fabricate 3D porous scaffolds. Conventional methods (e.g., salt leaching, solvent casting, phase inversion, etc.) are not capable of precisely controlling pore geometry, spatial distribution and interconnectivity [16,36,37]. On the other hand, additive manufacturing, also known as 3D printing or solid freeform fabrication, represents the key to fabricate customized and reproducible scaffolds [38]. Among these techniques, Fused Deposition Modeling (FDM) offers the opportunity to process highly filled composites, thus obtaining 3D morphologically controlled micro/nano-composite scaffolds. This technique involves a moving nozzle to extrude a fiber of polymeric or composite material by which the physical model is built layer-by-layer [16,20,37-41]. Conversely, stereolithography relies on the UV polymerization process. As in the case of FDM, stereolithography allows to process composite materials, but the amount of fillers is highly limited by the viscosity of the reactive photo-curable solution [16,36,42,43].

Recently, novel routes in tissue engineering have involved the use of magnetic nanoparticles (MNPs) to induce tissue growth through magnetic fields. Iron doped hydroxyapatite nanoparticles and iron oxide have been included into a polymeric matrix in order to guide bone regeneration [44-46]. The superparamagnetic feature of magnetic nanocomposite materials has allowed to develop an advanced and efficient *in vitro* method for the seeding of magnetically labeled cells, and a remarkable bone regeneration has been observed *in vivo* [47]. Moreover, this approach allows also to benefit from the effects of induced hyperthermia [48, 49].

In a joint connective tissues can be considered as composite materials mainly composed of collagen, hydroxyapatite and water-gel containing proteoglycans [50-52], and the time-dependent properties (viscoelasticity) of bone and cartilage are strongly related to the age, organ and district site [50,53-55]. On the other hand, mimicking of the mechanical and viscoelastic properties has shown to be very effective for improving the design of prosthetic [56,57] and scaffold devices [58]. Dynamic Mechanical Analysis (DMA) is a powerful tool to study the viscoelastic behavior of materials [8,50,53-55,57]. It is recognized that mechanisms occurring during tissue adaptation rely on a cellular mechanotransduction process driven by dynamic rather than static loading [59,61]. Of course, viscoelastic properties of scaffolds are of paramount importance especially in relation to the remarkable effects of dynamic mechanical stimulation, *in vivo* and *in vitro* through bioreactors, on tissue adaptation/regeneration [59-62].

Accordingly, through the combination of additive manufacturing approaches, the aim of the current research was the design and preparation of scaffolds for bone and cartilage regeneration, as well as the assessment of the viscoelastic features through DMA.

2. Materials and Methods

Poly(ε-caprolactone) (PCL) and PCL/MNPs nanocomposites scaffolds were fabricated through FDM technique (Fig. 1a), while poly(ethylene glycol) diacrylate (PEGDA) and PEGDA/MNPs scaffolds were manufactured

using stereolithography (Fig. 1b). 3D cylindrical hybrid scaffolds (Fig. 1c) were also obtained through a proper combination of these technologies.
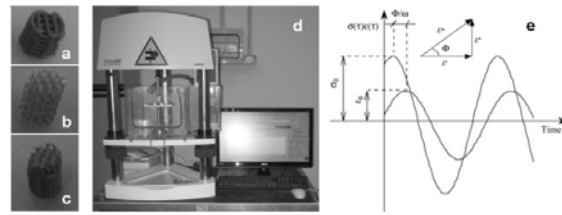

Fig. 1. (a) PCL/MNPs 80/20 scaffold obtained through FDM; (b) PEG/MNPs 95/5 scaffold obtained through stereolithography; (c) Multimaterial scaffold obtained combining stereolithography and FDM; (d) mechanical spectrometer equipped with a water bath at 37°C; (e) typical dynamic mechanical measurement and analysis for determining viscoelastic properties.

2.1. Scaffolds preparation: FDM

PCL pellets (M_w=65,000, Sigma-Aldrich, St. Louis, MO) and PCL/MNPs pellets were processed through FDM using a 3D plotter (Bioplotter, Envisiontec GmbH, Gladbeck, Germany) to manufacture 3D cylindrical scaffolds (6 mm in diameter, 8 mm in height) with a 0/0/90/90° lay-down pattern (Fig. 1a). PCL/MNPs pellets were obtained by dissolving PCL in tetrahydrofuran (THF, Sigma-Aldrich, St. Louis, MO) and adding MNPs and ethanol to the PCL/THF solution during stirring. Sonication through the ultrasonic bath (Branson 1510 MT, Danbury, CT) promoted the dispersion of the nanoparticles in the solution. The polymer/filler weight ratio (wt/wt) was 80/20.

The stainless steel injector of the FDM apparatus was pressurized to 8.5 bar and it was heated to a temperature of 90°C and 120°C for PCL and PCL/MNPs scaffolds, respectively. The material was deposited at a speed of 35 mm/min through a nozzle with an inner diameter of 600 µm.

2.2. Scaffolds preparation: stereolithography

PEGDA and PEGDA/MNPs photo-curable solutions were processed through stereolithography (Envisiontec Perfactory Mini Multilens SLA). Briefly, MNPs were dispersed in the monomer solution through sonication. PEG/MNPs 95/5 and PEG/MNPs 90/10 formulations were prepared, also including the photo-initiator Lucirin-TPO (4% wt).

Surfaces, which are periodic in three independent directions, were generated using K3DSurf v0.6.2 software, and diamond like architectures, according to the boundary conditions x^2+y^2:[-4π,4π] and z:[-8π,8π], were obtained using the following trigonometric functions:

$$\sin(x)\sin(y)\sin(z) + \sin(x)\cos(y)\cos(z) + \cos(x)\sin(y)\cos(z) + \cos(x)\cos(y)\sin(z) = C \quad (1)$$

where C is the offset value that regulates the porosity of the structure. This value was set at 0.4 to obtain a porosity of about 80%.

The building process involved projections of 1280*1024 pixels, each 32*32 μm^2 in size, and the layers thickness was 25 μm. Post-curing was carried out at 90°C for 1 day under vacuum. PEG, PEG/MNPs 95/5 and PEG/MNPs 90/10 scaffolds (Fig. 1b) were 3D manufactured.

2.3. Dynamic mechanical measurements

Dynamic mechanical tests in compression were carried out with a Bose Enduratec ELF 3200 (Minnetonka, USA) equipped with a water chamber controlled by a heater mixer (TE-10D Techne Cambridge, UK) (Fig. 1d). DMA, in a displacement control mode, was performed using sinusoidal waveforms between 0.01 and 100 Hz, thus spanning four frequency decades. The strain excitation signal (ε) is given by the ratio Δh/h₀, where h₀ is the specimen height, while the stress response is given by the ratio F/A, where F is the load and A is the "apparent" scaffold cross-section [16,46,49]. Dynamic data (Fig. 1e) were interpreted by means of phase angle (Φ) measurements, thus distinguishing the storage modulus (E') and the loss modulus (E''), defined as follows:

$$E' = \frac{\sigma_0}{\varepsilon_0} cos(\Phi) \qquad (2)$$

$$E'' = \frac{\sigma_0}{\varepsilon_0} sin(\Phi) \qquad (3)$$

Where σ_0 and ε_0 are the stress and the strain amplitudes, respectively.

2.4. SEM imaging

Scanning electron microscopy (SEM) was carried out to study morphology, pore shape and size of PCL and PEG based magnetic 3D scaffolds. The specimens were gold sputtered and analyzed through a FEI QUANTA 200 (The Netherlands, FEI Company) scanning electron microscope working at 30 kV.

3. Results and Discussion

Morphologically controlled scaffolds were fabricated through additive manufacturing techniques. From a static mechanical point of view, it was previously shown that PCL based scaffolds represent good candidates for bone regeneration [13,15,18,32,41] and the magnetic feature of PCL/MNPs scaffolds offered advanced opportunity to guide trabecular bone regeneration *in vitro* and *in vivo* [16, 44,47,50].
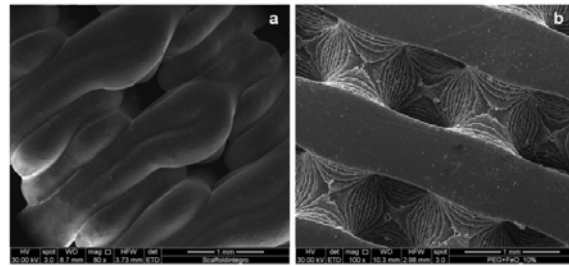

Fig. 2. (a) Architecture of PCL based magnetic 3D scaffold; (b) Architecture of PEG based magnetic 3D scaffold.

Figure 2 shows the morphology of PCL and PEG based magnetic nanocomposite scaffolds analyzed through SEM.

The obtained SEM results show that the designed scaffolds display a fully interconnected pore network, as well as a morphologically controlled architecture, highlighting the different morphology of the structures which should influence the mechanical and functional properties. The physical integrity of the filaments/fibers and layers was confirmed through SEM investigations, the pore shape and size obtained were consistent with the theoretical values defined during the design process. The 0/0/90/90° lay-down pattern (Fig. 2a) for the PCL based architecture obtained through FDM, and the layer stratification for PEG based architecture fabricated through stereolithography (Fig. 2b) at thickness of 25 μm, can be easily detected. Also, the periodic surface generating the PEG based scaffold can be easily distinguished.

The storage modulus of PCL based scaffold (Fig. 3) is almost constant between 0.01 Hz and 10 Hz, while it slightly increases (of about 10%) as the frequency increases from 1 Hz to 100 Hz, ranging from 68 MPa to78 MPa. A similar behavior was observed for PCL/MNPs 80/20 magnetic scaffolds, however showing higher values of storage modulus. These values increased from 99 MPa to 109 MPa as the frequency was increased from 0.01 Hz to 100 Hz. Therefore, as previously observed [44,47-50], MNPs represent an effective reinforcement for the PCL based architecture.

On the other hand, for both PCL and PCL/MNPs, the loss modulus is almost constant between 0.01 Hz and 1 Hz, while it remarkably increases through the last decade of the frequency sweep. In particular, the loss modulus for PCL based scaffolds spans from 3.4 MPa to 11.8 MPa, while it ranges between 5.7 MPa and 19.9 MPa for PCL/MNPs based scaffolds. Such values suggest that PCL based scaffolds have some capability to damp the mechanical vibrations. This capability has to be ascribed to the viscoelastic nature of PCL in the rubbery state at 37°C.

When using DMA to assess the viscoelastic properties of materials, the shock absorbing capability is directly related to the phase angle (Φ) measurements [8,55,57,63]. This measurement can be carried out independently of the specimen geometry by considering the shift angle between the applied sinusoidal displacement and the response in terms of force. This phase shift is related to the amount of energy that the structure is capable to dissipate. Furthermore, tan Φ represents the loss factor or loss tangent. For both the PCL and PCL/MNPs structures the loss factor increases from 0.04

to 0.18 as frequency increases. These values are consistent with loss factor measurements on subchondral bone of the human tibial plateau [55].
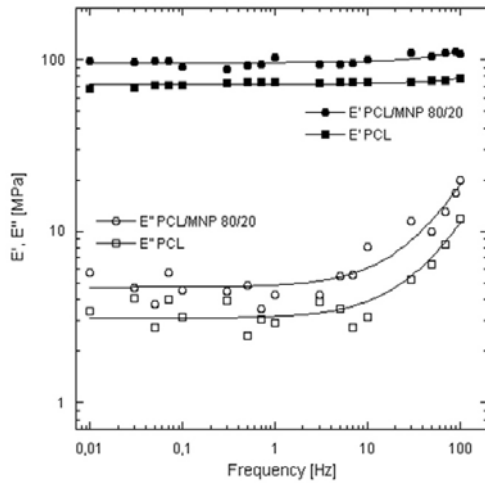

Fig. 3. Storage modulus (E') and loss modulus (E'') as function of frequency for PCL and PCL/MNPs 80/20 magnetic scaffolds.

It is worth noting that the storage modulus at 0.01 Hz of the subchondral bone of the human tibial plateau varies from 53 MPa to 230 MPa according to the site [50,55], and its values rise as frequency increases, analogously to PCL based scaffold. Furthermore, the loss modulus of the subchondral bone of the human tibial plateau at 0.01 Hz varies from 7.9 MPa to 50 MPa according to the site [54], and it increases as the frequency increases up to 100 Hz. Loss modulus for PCL based scaffolds are in the range of those from the tibial plateau. Therefore, the PCL based architectures obtained through FDM are very good candidate to mimic viscoelastic properties of subchondral bone.

The storage modulus of PEG based scaffold (Fig. 4) is almost constant between 0.01 Hz and 100 Hz. Higher values were measured for PEG/MNPs 95/5 scaffolds. The mean value storage modulus for PEG/MNPs 95/5 is 4.4 MPa, while those of PEG and PEG/MNPs 90/10 are similar (3.5 MPa). For all the scaffolds obtained through stereolithography, the loss modulus is almost constant up to 1Hz, while showing a consistent increase through the last two decades of the frequency sweep. In particular, the loss modulus spanned from 120 kPa to 250 kPa, from 80 kPa to 250 kPa and from 80 kPa to 140 kPa for PEG, PEG/MNPs 95/5 and PEG/MNPs 90/10 structures, respectively. Therefore, it is also interesting to note that PEG/MNPs 90/10 scaffold have shown lower damping properties.
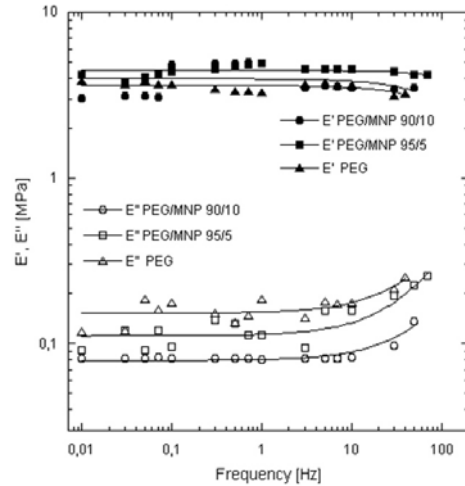

Fig. 4. Storage modulus (E') and loss modulus (E'') as function of frequency for PEG, PEG/MNPs 95/05 and PEG/MNPs 90/10 magnetic scaffolds.

It is remarkable to report that the storage modulus of bovine articular cartilage tested at 37°C increases from 470 kPa at 0.1 Hz to 1 MPa at 10 Hz [53] while higher but almost constant values have been observed at room temperature at high frequency [54]. Therefore, the storage moduli of the PEG based scaffolds (Fig. 3) are comparable to those of articular cartilage. The loss modulus of bovine articular cartilage tested in wet environment at 37°C has shown to be almost constant in the frequency range of 0.1-10 Hz, varying between 176 kPa and 249 kPa [53]. Consequently, also the loss modulus of the PEG based scaffolds (Fig. 3) are in the range of those measured for the articular cartilage [53]. In particular, for all the PEG based scaffolds, the phase angle (Φ) spanned from 1.0° to 9.8°, showing a mean value of 4.0°. Also these value are in agreement with phase angle measurements of bovine articular cartilage [54].

As previously reported [44,47], a 3D superparamagnetic scaffold can be considered as a fixed 'station', incorporating a programmed biofactor release, triggered by external magnetic fields. The incorporation of MNPs in PEG- and PCL-based scaffolds strongly influences viscoelastic properties. Static mechanical analyses have shown that, for PCL scaffold [44,47,50], the inclusion of MNPs results in an improvement of the elastic modulus, however decreasing their ductility. From a dynamic point of view, storage modulus profiles obtained at 37°C (Fig. 3) confirm the strengthening effect of MNPs. This result can be ascribed to the difference in the stiffness and ductility between the polymeric matrix and purely inorganic nanoparticles. Hence, these differences influence the viscoelastic behaviour during compression.

Instead, for PEG based scaffolds, MNPs seems to be an effective reinforcement only up to 5% by weight. The lower storage modulus recorded for the PEG/MNPs 90/10 scaffolds may be due to a clustering effect of MNPs occurring in the monomer solution undergoing the step by step photo-polymerization process. Therefore, the lower values of the

storage modulus at high MNP amount can be ascribed to the poor interface between clusters and polymeric matrix.

It has been suggested that tissue remodelling, adaptation and regeneration is mainly driven by dynamic rather than static stimulation [59-62]. In particular, models of bone adaptation in a rat ulna suggests that the dissipation energy stimulus plays a crucial role for tissue growth [61]. Of course, for regeneration through the tissue engineering approach, this stimulus depends on scaffold viscoelasticity. Even if some class of metals used for biomedical application, such as shape memory alloys based on titanium, displays marked time- and temperature-dependent properties [63-65], polymer based composite scaffolds can be considered ideal materials for reproducing viscoelastic properties of natural tissues [25,57], and the viscoelastic properties measured for PEG and PCL based scaffolds should promote an efficient mechanotransduction [59-63]. Moreover, as reported in the literature, it is possible to adopt different strategies for surface functionalization of the selected polymers, in order to improve cell-material interaction [32-35]. The fully interconnected porosity of PEG and PCL based scaffolds also allows to benefit from injectable gel based formulation [26-30] capable to release, *in situ*, drugs or cells [30,31]. In particular, for superparamagnetic scaffolds, it has already been shown that enhanced gel infiltration [31] or cell seeding [47] into the scaffold can be achieved through the use of an external magnetic field.

Osteoarthritis is a degenerative joint disease that mainly affects the knee and hip especially for the elderly population. In the late stage, patients affected by this disease show severe pain and the restriction of their daily activities [1-4]. Total joint arthroplasty actually represents the method of choice for the treatment of late stage osteoarthritis. This method involves the use of prostheses made of non-degradable biomaterials such as metals, ceramics, polymers and composites [4-7]. Among the drawbacks, stress-shielding effects due to the stiffness of these prosthetic materials, higher than that of the hosting bone, determine tissue resorption around the prosthesis. Fatigue, corrosion, wear and debris are further drawbacks, and finally aseptic loosening [4], hence, a revision of the implant is a demand [10]. Consequently, regeneration of osteochondral bone represents an important goal, and our results suggest that a multimaterial scaffold based on PCL and PEG loaded with MNPs, fabricated by combining stereolithography and FDM techniques, may adequately reproduce viscoelastic properties of osteochondral tissues.

4. Conclusions

PCL and PEG based magnetic nanocomposite scaffolds adequately reproduce viscoelastic properties of trabecular bone and articular cartilage tissues, respectively. By combining fused deposition modeling and stereolithography it is possible to fabricate a hybrid multimaterial scaffold suitable for osteochondral tissue regeneration.

References

[1] Peat G, McCarney R, Croft P. Knee pain and osteoarthritis in older adults: a review of community burden and current use of primary health care. Ann Rheum Dis 2001;60:91-97.

[2] Wallis JA, Taylor NF. Pre-operative interventions (non-surgical and non-pharmacological) for patients with hip or knee osteoarthritis awaiting joint replacement surgery - a systematic review and meta-analysis. Osteoarthritis Cartilage 2011;19:1381-95.

[3] Spahn G, Hofmann GO, von Engelhardt LV, Li M, Neubauer H, Klinger HM. The impact of a high tibial valgus osteotomy and unicondylar medial arthroplasty on the treatment for knee osteoarthritis: a meta-analysis. Knee Surg Sports Traumatol Arthrosc 2013;21:96-112.

[4] Ronca D, Guida G. Knee Joint Replacements. In: Barbucci R, editors. Integrated Biomaterials Science Springer US: Kluwer Academic Publishers 2002. p. 527-554

[5] De Santis R, Gloria A, Ambrosio L. Composite materials for hip joint prostheses. In: Ambrosio L editors. Biomedical Composites. Boston: CRC Press, Woodhead Publishing Limited 2010. p. 276-295.

[6] Merolli A, Perrone V, Tranquilli Leali P, Ambrosio L, De Santis R, Nicolais L, Gabbi C. Response to polyetherimide based composite materials implanted in muscle and in bone. J Mater Sci Mater Med 1999;10:265-8.

[7] De Santis R, Ambrosio L, Nicolais L. Polymer-based composite hip prostheses. J Inorg Biochem. 2000;79:97-102.

[8] De Santis R, Mollica F, Ambrosio L, Nicolais L, Ronca D. Dynamic mechanical behavior of PMMA based bone cements in wet environment. J Mater Sci Mater Med 2003;14:583-94.

[9] De Santis R, Ambrogi V, Carfagna C, Ambrosio L, Nicolais L. Effect of microencapsulated phase change materials on the thermo-mechanical properties of poly(methyl-methacrylate) based biomaterials. J Mater Sci Mater Med 2006 ;17:1219-26.

[10] Nizard RS, Sedel L, Christel P, Meunier A, Soudry M, Witvoet J. Ten-year survivorship of cemented ceramic-ceramic total hip prosthesis. Clin Orthop Relat Res 1992;53-63.

[11] Klein-Nulend J, Bacabac RG, Mullender MG. Mechanobiology of bone tissue. Pathol Biol Paris 2005;53:576-80.

[12] Rezwan K, Chen QZ, Blaker J J, Boccaccini AR. Biodegradable and bioactive porous polymer/inorganic composite scaffolds for bone tissue engineering. Biomaterials 2006;27:3413-31.

[13] De Santis R, Gloria A, Russo T, D'Amora U, D'Antò V, Bollino F, Catauro M, Mollica F, Rengo S, Ambrosio L. PCL loaded with sol–gel synthesized organic–inorganic hybrid fillers: From the analysis of 2D substrates to the design of 3D rapid prototyped composite scaffolds for tissue engineering. AIP Conf Proc 2012;1459:26-29.

[14] Hollister SJ. Porous scaffold design for tissue engineering. Nat Mater 2005;4:518-524.

[15] Russo T, Gloria A, D'Antò V, D'Amora U, Ametrano G, Bollino F, De Santis R, Ausanio G, Catauro M, Rengo S, Ambrosio L. Poly(ε-caprolactone) reinforced with sol–gel synthesized organic–inorganic hybrid fillers as composite substrates for tissue engineering. J Appl Biomater Biomech 2010;8:146-52.

[16] Gloria A, De Santis R, Ambrosio L. Polymer-based composite scaffolds for tissue engineering. J Appl Biomater Biomech 2010;8:57-67.

[17] De Santis R, Gloria A, Russo T, D'Amora U, D'Antò V, Bollino F, Catauro M, Mollica F, Rengo S, Ambrosio L. Advanced composites for hard-tissue engineering based on PCL/organic–inorganic hybrid fillers:

From the design of 2D substrates to 3D rapid prototyped scaffolds. Polymer Composites 2013;34:1413-1417.

[18] Gloria A, Ronca D, Russo T, D'Amora U, Chierchia M, De Santis R, Nicolais L, Ambrosio L. Technical features and criteria in designing fiber-reinforced composite materials: from the aerospace and aeronautical field to biomedical applications. J Appl Biomater Biomech 2011;9:151-163.

[19] Puppi D, Mota C, Gazzarri M, Dinucci D, Gloria A, Myzabekova M, Ambrosio L, Chiellini F. Additive manufacturing of wet-spun polymeric scaffolds for bone tissue engineering. Biomedical Microdevices 2012;14:1115-1127.

[20] Kyriakidou K, Lucarini G, Zizzi A, et al. Dynamic co-seeding of osteoblast and endothelial cells on 3D polycaprolactone scaffolds for enhanced bone tissue engineering. Journal of Bioactive and Compatible Polymers 2008; 23: 227-43.

[21] Gloria A, Causa F, Russo T, Battista E, Della Moglie R, Zeppetelli S, De Santis R, Netti PA, Ambrosio L. Three-Dimensional Poly(ε-caprolactone) Bioactive Scaffolds with Controlled Structural and Surface Properties. Biomacromolecules 2012;13:3510-21.

[22] Gloria A, De Santis R, Ambrosio L, Causa F, Tanner KE. A multi-component fiber-reinforced PHEMA-based hydrogel/HAPEX™ device for customized intervertebral disc prosthesis. J Biomater Appl 2011;25:795-810.

[23] Esposito AR, Moda M, de Melo Cattani SM, de Santana GM, Abreu Barbieri J, Moron Munhoz M, Pereira Cardoso T, Peris Barbo ML, Russo T, D'Amora U, Gloria A, Ambrosio L, de Rezende Duek EA. PLDLA/PCL-T Scaffold for Meniscus Tissue Engineering. BioRes Open Access 2013;2:138-147.

[24] Antunes JC, Pereira CL, Molinos M, Ferreira da Silva F, Dessì M, Gloria A, Ambrosio L, Gonçalves RM, Barbosa MA. Layer-by-Layer Self-Assembly of Chitosan and Poly(γ-glutamic acid) into Polyelectrolyte Complexes. Biomacromolecules 2011;12:4183 4195.

[25] Silva-Correia J, Gloria A, Oliveira MB, Mano JF, Oliveira JM, Ambrosio L, Reis RL. Rheological and mechanical properties of acellular and cell-laden methacrylated gellan gum hydrogels. J Biomed Mater Res A 2013; 101: 3438-46.

[26] Reitmaier S, Wolfram U, Ignatius A, Wilke HJ, Gloria A, Martín-Martínez JM, Silva-Correia J, Oliveira JM, Reis RL, Schmidt H. Hydrogels for nucleus replacement – facing the biomechanical challenge. J Mech Behav Biomed Mater 2012; 14: 67-77.

[27] Giordano C, Albani D, Gloria A, Tunesi M, Batelli S, Russo T, Forloni G, Ambrosio L, Cigada A. Multidisciplinary perspectives for Alzheimer's and Parkinson's diseases: hydrogels for protein delivery and cell-based drug delivery as therapeutic strategies. Int J Artif Organs 2009; 32: 836-850.

[28] Giordano C, Albani D, Gloria A, Tunesi M, Rodilossi S, Russo T, Forloni G, Ambrosio L, Cigada A. Nanocomposites for neurodegenerative diseases: hydrogel-nanoparticle combinations for a challenging drug delivery. Int J Artif Organs 2011; 34: 1115-27.

[29] Meikle ST, Standen G, Salvage J, De Santis R, Nicolais L, Ambrosio L, Santin M. Synthesis and characterization of soybean-based hydrogels with an intrinsic activity on cell differentiation. Tissue Eng Part A 2012;18:1932-9.

[30] Tsaryk R, Gloria A, Russo T, Anspach L, De Santis R, Ghanaati S, Unger RE, Ambrosio L, Kirkpatrick CJ. Collagen-low molecular weight hyaluronic acid semi-interpenetrating network loaded with gelatin microspheres for cell and growth factor delivery for nucleus pulposus regeneration. Acta Biomaterialia 2015;20:10–21.

[31] Russo T, D'Amora U, Gloria A, Tunesi M, Sandri M, Rodilossi S, Albani D, Forloni G, Giordano C, Cigada A, Tampieri A, De Santis R, Ambrosio L. Systematic Analysis of Injectable Materials and 3D Rapid Prototyped Magnetic Scaffolds: From CNS Applications to Soft and Hard Tissue Repair/Regeneration. Procedia Eng 2013; 59: 233–239.

[32] Domingos M, Intranuovo F, Gloria A, Gristina R, Ambrosio L, Bártolo PJ, Favia P. Improved osteoblast cell affinity on plasma-modified 3D-extruded PCL scaffolds. Acta Biomaterialia 2013;9:5997-6005.

[33] Russo L, Russo T, Battocchio C, Taraballi F, Gloria A, D'Amora U, De Santis R, Polzonetti G, Nicotra F, Ambrosio L, Cipolla L. Galactose grafting on poly(ε-caprolactone) substrates for tissue engineering: a preliminary study. Carbohydr Res 2015;405:39-46.

[34] Guarino V, Gloria A, M. Alvarez-Perez A, Raucci MG, Cirillo V, Ronca A, De Santis R, Ambrosio L. Design of Functional Polymer and Composite Scaffolds for the Regeneration of Bone, Menisci, Osteochondral and Peripheral Nervous Tissues. Advanced Materials Research 2011;324:8-13.

[35] Dessì M, Alvarez-Perez MA, De Santis R, Ginebra MP, Planell JA, Ambrosio L. Bioactivation of calcium deficient hydroxyapatite with foamed gelatin gel. A new injectable self-setting bone analogue. J Mater Sci Mater Med 2014;25:283-95.

[36] Sachlos E, Czernuske JT. Making tissue engineering scaffold work: review on the application of SFF technology to the production of tissue engineering scaffolds. Eur Cell Mat 2003;5:29-40.

[37] Hutmacher DW, Schantz T, Zein I, Ng KW, Teoh SH, Tan KC. Mechanical properties and cell cultural response of polycaprolactone scaffolds designed and fabricated via fused deposition modelling. J Biomed Mater Res 2001;55:203-16.

[38] Santos ARC, Almeida HA, Bartolo PJ. Additive manufacturing techniques for scaffold-based cartilage tissue engineering. Virtual Phys Prototyp 2013; 8:175-86

[39] Domingos M, Chiellini F, Gloria A, Ambrosio L, Bartolo P, Chiellini E. Effect of process parameters on the morphological and mechanical properties of 3D Bioextruded poly(ε-caprolactone) scaffolds. Rapid Prototyp J 2012; 18: 56–67.

[40] Zein I, Hutmacher DW, Tan KC, Teoh SH. Fused deposition modeling of novel scaffold architectures for tissue engineering applications. Biomaterials 2002; 1169-85.

[41] Domingos M, Intranuovo F, Russo T, De Santis R, Gloria A, Ambrosio L, Ciurana J, Bartolo P. The first systematic analysis of 3D rapid prototyped poly(ε-caprolactone) scaffolds manufactured through BioCell printing: the effect of pore size and geometry on compressive mechanical behaviour and in vitro hMSC viability. Biofabrication 2013; 5: 045004-1-045004-13.

[42] Peltola SM, Melchels FPW, Grijpma DK, Kellomäki M. A review of rapid prototyping techniques for tissue engineering purposes. Ann Med 2008; 40: 268-80.

[43] Ronca A, Ambrosio L, Grijpma DW. Design of porous three-dimensional PDLLA/nano-hap composite scaffolds using stereolithography. J Appl Biomater Funct Mater 2012;10:249-58.

[44] Gloria A, Russo T, D'Amora U, Zeppetelli S, D'Alessandro T, Sandri M, Bañobre-López M, Piñeiro-Redondo Y, Uhlarz M, Tampieri A, Rivas J, Herrmannsdörfer T, Dediu VA, Ambrosio L, De Santis R. Magnetic poly (ε-caprolactone)/iron-doped hydroxyapatite nanocomposite substrates for advanced bone tissue engineering. J R Soc Interf 2013;10: 20120833.

[45] De Santis R, Gloria A, Russo T, D'Amora U, Zeppetelli S, Tampieri A, Herrmannsdörfer T, Ambrosio L. A route toward the development of 3D magnetic scaffolds with tailored mechanical and morphological properties for hard tissue regeneration: preliminary study. Virtual and Physical Prototyping 2011;6:189-195.

[46] De Santis R, Gloria A, Russo T, D'Amora U, Zeppetelli S, Dionigi C, Sytcheva A, Herrmannsdörfer T, Dediu V Ambrosio L. A basic approach toward the development of nanocomposite magnetic scaffolds for advanced bone tissue engineering. J Appl Pol Sci 2011; 122: 3599-3605.

[47] De Santis R, Russo A, Gloria A, D'Amora U, Russo T, Panseri S, Sandri M, Tampieri A, Marcacci M, Dediu VA, Wilde CJ.; Ambrosio L. Towards the Design of 3D Fiber-Deposited Poly(ε-caprolactone)/Iron-Doped Hydroxyapatite Nanocomposite Magnetic Scaffolds for Bone Regeneration. Journal of Biomedical Nanotechnology 2015;11:1236-1246.

[48] Banobre-Lopez M, Pineiro-Redondo Y, De Santis R, Gloria A, Ambrosio L, Tampieri A, Dediu V, Rivas J. Poly (caprolactone) based magnetic scaffolds for bone tissue engineering. J Appl Phys 2011;109: 07B313-1-07B313-3.

[49] Banobre-Lopez M, Pineiro-Redondo Y, Sandri M, Tampieri A, De Santis R, Dediu VA, Rivas J. Hyperthermia Induced in Magnetic Scaffolds for Bone Tissue Engineering. Magnetics, IEEE Transactions 2014;50: 1-7.

[50] De Santis R, Ambrosio L, Mollica F, Netti P, Nicolais L. Mechanical properties of human mineralized connective tissues. Modeling of Biological Materials. In: Mollica F, Preziosi L, Rajagopal KR, editors. Modeling of Biological Materials. Boston: Birkhäuser; 2007. p. 211-261.

[51] Dunn MG, Silver FH. Viscoelastic behavior of human connective tissues: relative contribution of viscous and elastic components. Connect Tissue Res 1983;12:59-70.

[52] De Santis R, Ambrosio L, Nicolais L. Mechanical properties of tooth structures. In: Barbucci R, editors. Integrated Biomaterials Science. Springer US: Kluwer Academic Publishers 2002. p. 589-599.

[53] Schwartz CJ, Bahadur S. Investigation of articular cartilage and counterface compliance in multi-directional sliding as in orthopedic implants. Wear 2007; 262:1315–1320.

[54] Fulcher GR, Hukins DW, Shepherd DE. Viscoelastic properties of bovine articular cartilage attached to subchondral bone at high frequencies. BMC Musculoskelet Disord 2009;4:10:61.

[55] Ronca D, Gloria A, De Santis R, Russo T, D'Amora U, Chierchia M, Nicolais L, Ambrosio L. Critical analysis on dynamic-mechanical performance of spongy bone: the effect of an acrylic cement. Hard Tissue 2014;3:9-15.

[56] Ambrosio L, De Santis R, Iannace S, Netti PA, Nicolais L. Viscoelastic behavior of composite ligament prostheses. J Biomed Mater Res 1998;42:6-12.

[57] Gloria A, Causa F, De Santis R, Netti PA, Ambrosio L. Dynamic-mechanical properties of a novel composite intervertebral disc prosthesis. J Mater Sci Mater Med 2007;18:2159-65.

[58] Borzacchiello A, Gloria A, Mayol L, Dickinson S, Miot S, Martin I, Ambrosio L. Natural/synthetic porous scaffold designs and properties for fibro-cartilaginous tissue engineering. Journal of Bioactive and Compatible Polymers 2011;26:437-451.

[59] Turner CH, Pavalko FM. Mechanotransduction and functional response of the skeleton to physical stress: the mechanisms and mechanics of bone adaptation . J Orthop Sci 1998;3:346-55.

[60] Gross TS, Srinivasan S, Liu CC, Clemens TL, Bain SD. Noninvasive loading of the murine tibia: an in vivo model for the study of mechanotransduction . J Bone Miner Res 2002 ;17(3):493-501.

[61] Chennimalai Kumar N, Dantzig JA, Jasiuk IM. Modeling of cortical bone adaptation in a rat ulna: effect of frequency. Bone 2012;50:792-7.

[62] Lee J, Guarino V, Gloria A, Ambrosio L, Tae G, Kim YH, Jung Y, Kim SH, Kim SH. Regeneration of Achilles' tendon: the role of dynamic stimulation for enhanced cell proliferation and mechanical properties. J Biomater Sci Polym Ed 2010;21:1173-90.

[63] Laino G, De Santis R, Gloria A, Russo T, Quintanilla DS, Laino A, Martina R, Nicolais L, Ambrosio L. Calorimetric and thermomechanical properties of titanium-based orthodontic wires: DSC-DMA relationship to predict the elastic modulus. J Biomater Appl. 2012;26:829-44.

[64] De Santis R1, Dolci F, Laino A, Martina R, Ambrosio L, Nicolais L. The Eulerian buckling test for orthodontic wires. Eur J Orthod. 2008;30:190-8.

[65] El Feninat F, Laroche G, Fiset M, Mantovani, D. Shape Memory Materials for Biomedical Applications. Adv Eng Mater 2002;4:91-104.